SUPPLEMENTAL MATERIALS

Direct correlation between creep compliance and deformation in entangled and sparsely crosslinked microtubule networks

By Yali Yang, Jun Lin, Bugra Kaytanli , Omar A. Saleh, and Megan T. Valentine

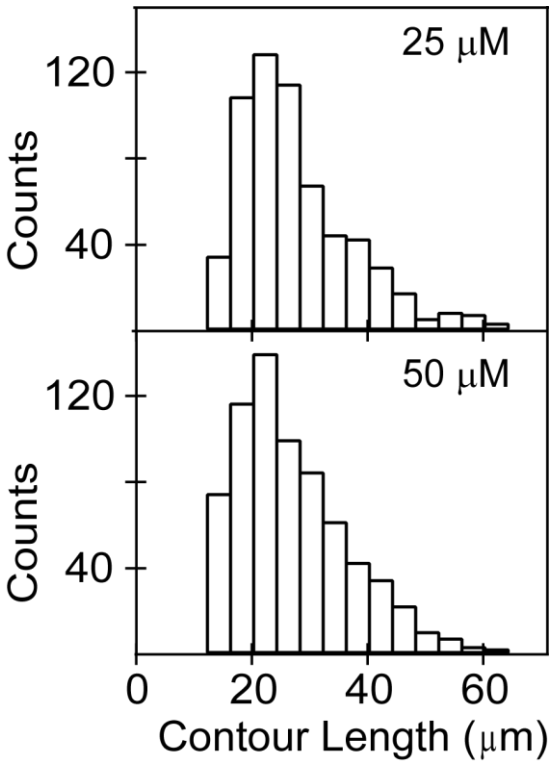

Figure S1:. Contour length distribution for MTs is independent of tubulin concentration. The distribution of MT lengths is determined by attaching individual MTs to a coverslip, visualizing them using TIRF microscopy, and measuring their lengths manually using built-in measurement tools in ImageJ. Under the polymerization conditions used for this work, we find the length distribution to be constant as a function of tubulin concentration. The mean length for 25 μM tubulin is 23.9 ± 0.4 μm (SEM; 623 measurements) and for 50 μM tubulin is 23.3 ± 0.4 μm (SEM; 710 measurements), as shown.

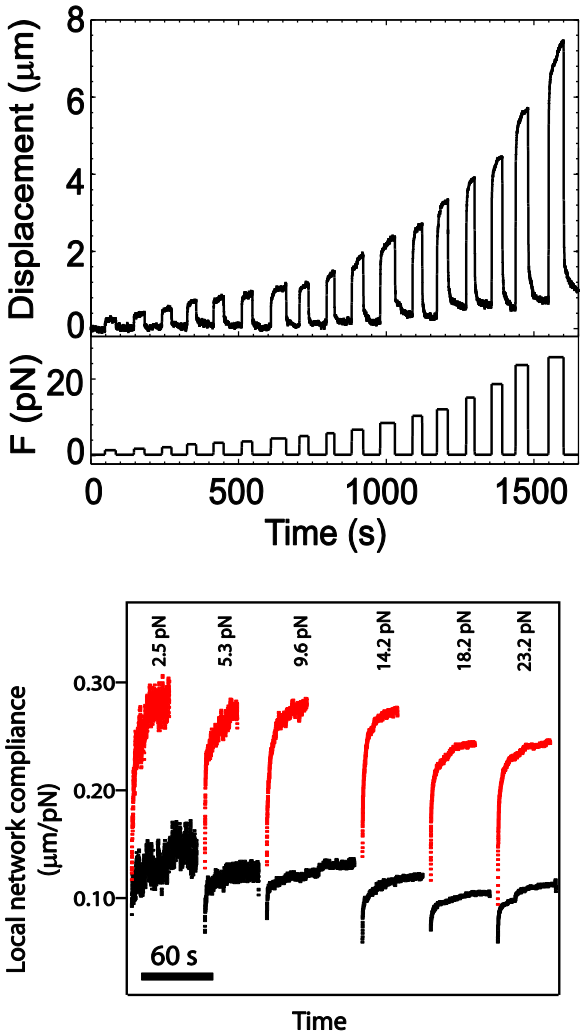

Figure S2: Representative traces showing force-dependent bead displacement as a function of time. (Top) Force is ramped up from ~1–33 pN over the course of the measurement, which typically takes ~20-30 minutes per bead. For small forces the response is typically elastic: bead position is approximately constant under constant force, and the bead returns to its original position when the force is stepped down to zero. At larger forces, a creep regime is observed, in which the bead position increases linearly with time. When creep is observed, the bead does not fully return to its starting position, due to energy dissipation and interactions with microstructure. (Bottom) The local network compliance can be determined by dividing the bead displacement by the applied force, as shown for a sampling of forces for entangled (red) and crosslinked (black) networks of 26 μM tubulin. Each trace shows the behaviour of a single bead under force. The compliance is roughly constant for the entangled networks for forces below ~ 15 pN, then decreases slightly, as expected for a stress-stiffening gel. The crosslinked networks are less compliant (stiffer) and less force sensitive.

.

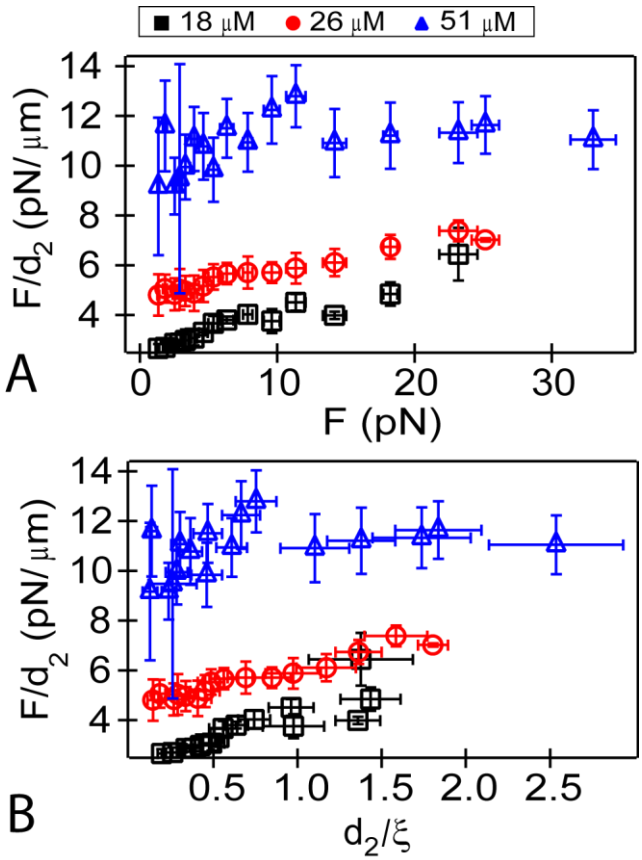

Figure S3: Stiffness of entangled MT networks, given by F/d_2 as a function of (A) force and (B) strain, d_2/ξ. Overall, the trends for the force off transition are similar to that of the force on transition (as shown in Figure 3). There is a low force plateau, in which stiffness values increase linearly with tubulin concentration, followed by a stiffening regime at high force (or strain). In detail, the onset of non-linearity differs from that of the force-on transition data, in which all networks stiffen above strains of ~ 70%. For the force-off transition, we find that the 18 μM (□) and 26 μM (○) networks start to stiffen at strains of ~ 30%, whereas the 51 μM (△) network response is linear across the range of forces probed.

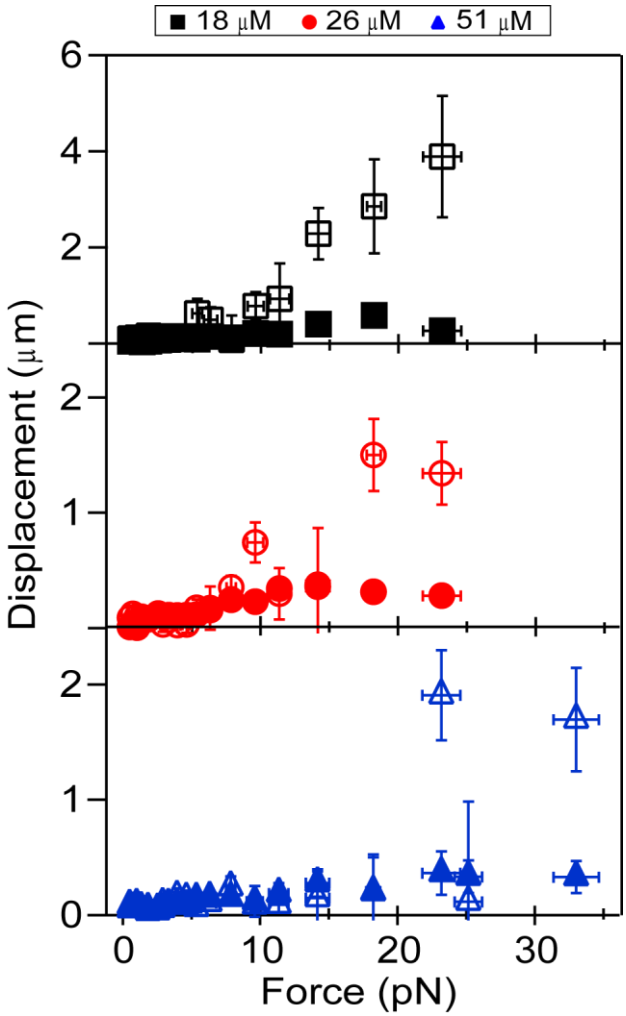

Figure S4: Comparison of the creep displacement Δx_c (solid symbols) to the unrecovered displacement Δx_f (open symbols). As expected from our analysis of the creep velocity, Δx_c increases monotonically with applied force. For small forces, $\Delta x_f \approx \Delta x_c$. At larger forces, $\Delta x_f >> \Delta x_c$ due to force-induced slippage of the bead through the porous network, which allows some beads to become trapped in new "pores" when the force is turned off. This behaviour is observed at all tubulin concentrations; however, higher forces are required to induce bead entrapment in denser networks.

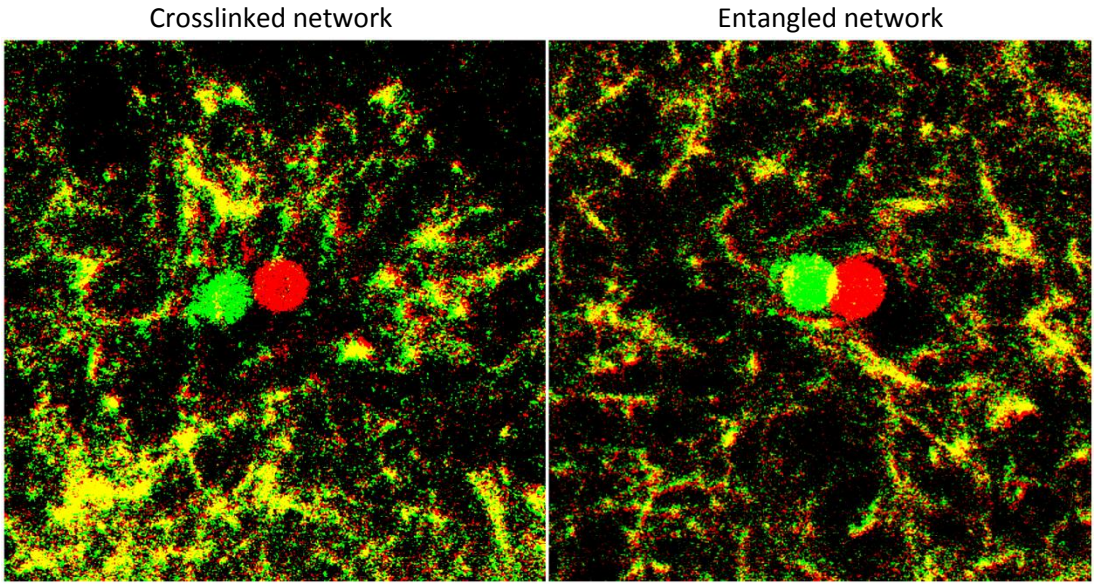

Figure S5 : Dual color images of networks showing force-induced network displacement. Here, representative images of weakly crosslinked (right) and entangled (left) 25 mM tubulin networks are shown. Each image is an overlay of an image collected under no force (red) and a second image collected under the application of ~25 pN force, which causes the bead and the entrained network to move toward the left (green). In places where the network is stationary upon application of force, the green and red images overlap and the composite image appears yellow. In the entangled case, the motion of the network is limited to the area just surrounding the bead, and highly bent filaments can be observed. By contrast, in the crosslinked cases, a much larger deformation zone extends for several particle diameters, and the filaments tend to collectively stretch rather than locally bend, indicating a more affine deformation field.

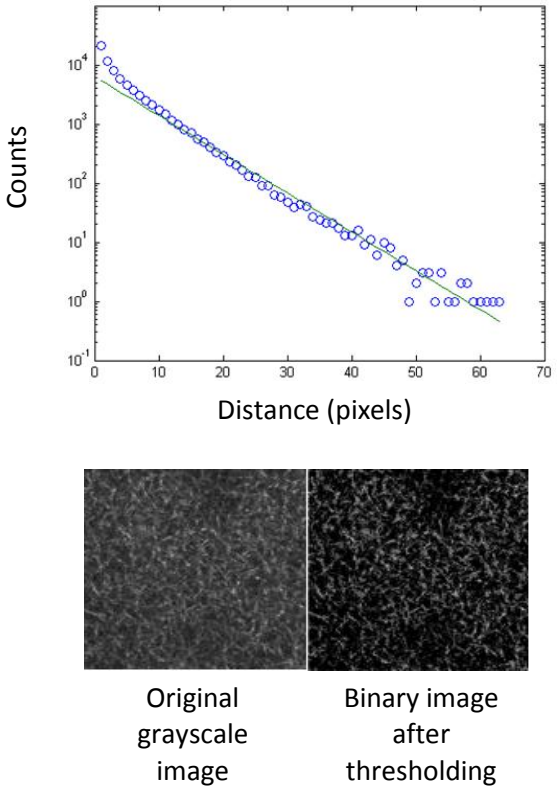

Figure S6 : Example of raw data used for mesh size determination. To quantify the mesh size of the MT networks, image analysis is performed on two-dimensional confocal images. After thresholding, the distance between nearest neighbour MT pixels within each row and column of the binary image is determined. Here, two sample images (~ 65 × 65 μm^2 field of view) are shown. This analysis is similar to calculating the radial distribution of distances between filament intersections, but is implemented in Cartesian coordinates to take advantage of the natural axes of the microscope images. The distribution of distances is plotted and fitted to an exponential $P(\xi) = P_0 e^{-r/\xi}$, where r is the distance between pixels and ξ is the characteristic mesh size. There is a systematic deviation at the smallest displacements due to the limited resolution of the microscope. This method has been used extensively in characterizing the structural properties of collagen and other extracellular matrix protein networks.